

## FINITE PLASTIC STRAIN IN ANNEALED COPPER DURING NON-PROPORTIONAL LOADING

JAMES F. BELL

Department of Mechanics, The Johns Hopkins University, Baltimore, MD 21218, U.S.A.

and

AKHTAR S. KHAN

School of Aerospace, Mechanical and Nuclear Engineering, The University of Oklahoma, Norman,  
OK 73069, U.S.A.

(Received 25 October 1979)

**Abstract**—In this paper it is shown that experimental results obtained for finite plastic strain produced by widely different non-proportional loading paths in annealed copper are in close accord with a recently developed incremental theory of finite strain plasticity. The measured strain components exceed 30%. Some attention also is given to the magnitude of the error introduced by a deformation theory approximation.

### INTRODUCTION

For over a century the purity and preparation of copper have been carefully controlled to maintain technologically important electrical properties; hence, it is a particularly suitable solid for the study of deformation, whether small or finite. Test data from the mid and late 19th century may be compared with experimental data from the eight decades of the 20th century. One of the present authors in tracing the history of large deformation in this interesting solid has found reproducible results for simple loading to finite strain extending back to the 1840's [1]. In the present series of experiments in annealed copper the emphasis is upon the study of finite deformation during more complex, non-proportional loading.

The specimens are thin-walled tubes of 99.9% pure copper with a 4 in. (101.6 mm) long test section, a 0.375 in. (9.525 mm) inside diameter and either a 0.415 in. (10.541 mm) or a 0.440 in. (11.176 mm) outside diameter. The tubes were annealed for one hour in an oxygen free atmosphere at 1100°F and cooled in the furnace over the next 24 hr. The dead-weight tension-torsion apparatus permitted the application of loads by means of water flowing from a constant head, producing arbitrary constant stress rates in tension and in torsion. The tensile strain was determined by two clip gages, attached opposite to each other; the shear angle was determined by direct optical measurement. The tension-torsion apparatus is the same as that initially developed by Mittal [2] and later modified by Moon [3]. The details are in those references and therefore are not given here.

The interest in the present study was in the finite strain response during loading for a generalized scalar measure of stress  $T$ , where  $dT \geq 0$ .

### EXPERIMENT AND FINITE STRAIN THEORY

The present paper will present a detailed experimental study of the dependence of finite deformation upon the character of the non-proportional loading path. The incremental theory of finite strain plasticity, referred to the undeformed reference configuration of the solid, was developed by Bell [4]. The results for proportional loading given in 1973 were extended in 1975 to include non-proportional loading [5]. In the following years Bell presented the theory in a completely general form, based upon experimentation not only in fully annealed, ordered, relatively pure solids but also for the finite strain of several structural metal alloys of aluminum, steel and copper [6-8]. Since the present study is for arbitrary non-proportional loading paths in the tension and torsion of thin-walled tubes, the constitutive statements of Bell's general theory are presented here only in those special terms.

Let  $\sigma = \text{axial force}/A_0$  be the nominal axial stress, with  $A_0$  the original measured cross-sectional area of the thin-walled tube;  $S = \text{torque}/r_m A_0$  be the nominal torsional shear

stress, where  $r_m$  is the initial mean radius of the thin-walled tube;  $\epsilon = (l - l_0)/l_0$  where  $l_0$  is the initial undeformed axial length and  $l$  is the measured axial length of the specimen during deformation; and  $s = r_m\theta/l_0$ , the nominal shear strain, with  $\theta$  the measured angle in radians during finite strain. All of the tests considered here are dead-weight loading measurements in which  $\sigma$  and  $S$  are prescribed. It is important that in this experiment the tension and torsional systems are decoupled. The axial load does not rotate during torsional straining and the axial strain component  $\epsilon$  is measured independent of the rotations  $\theta$  of the torsional strain  $s$ .

Motivated by what had been observed earlier during the finite strain of many solids, let the generalized scalar measure of stress be  $T = \sqrt{[(2/3)\sigma^2 + 2S^2]}$ . Those same experiments demonstrated definitively that in non-proportional loading a generalized finite strain  $\Gamma$  is path dependent [5-8]. Success in comparing experiment and theory was achieved with the introduction of the incremental generalized strain,  $d\Gamma = \sqrt{[3/2(d\epsilon)^2 + 1/2(ds)^2]}$ . Experiments on many solids showed that the generalized stress and strain for any arbitrary loading path, whether proportional or non-proportional, is given by eqn (1) for finite strain

$$d\Gamma = \frac{2T dT}{\beta^2} \quad \text{for } T > T_Y \quad (1)$$

where  $\beta$  is a measured material constant, and  $T_Y$  is the elastic limit of the solid.

For the specific situation of the tension and torsion of thin-walled tubes, constitutive equations which were found to be compatible with observed paths in strain space and consistent with the observed parabolicity of the generalized stress  $T$  and the generalized strain  $\Gamma$  are given by eqns (2) and (3). The introduction of these equations in  $d\Gamma$  of eqn (1) results in the right hand side of eqn (1); thus, all three of these equations are consistent

$$d\epsilon = \frac{4\sigma dT}{3\beta^2} \quad (2)$$

$$ds = \frac{4S dT}{\beta^2} \quad (3)$$

where

$$dT = \frac{\frac{2}{3}\sigma d\sigma + 2S dS}{T}.$$

For proportional loading, the generalized finite strain  $\Gamma$  depends only upon the current magnitude of the strain components, as  $\Gamma = \sqrt{[(3/2)\epsilon^2 + (1/2)s^2]}$  and the constitutive statements of eqns (2) and (3) may be readily integrated to provide eqns (4) and (5).

$$\epsilon = \frac{2\sigma T}{3\beta^2} + \epsilon_b \quad (4)$$

$$s = \frac{2ST}{\beta^2} + s_b \quad (5)$$

where  $\epsilon_b$  and  $s_b$  are intercepts on the strain axes for zero stress.

In all of the quasi-static, finite strain experiments on annealed copper tubes described in the present paper, the stress rates  $\dot{\sigma}$  and  $\dot{S}$  are constant during deformation.

First, as illustrative of the correlation obtainable between the finite strain theory and experiment for *proportional* loading, experimental results for simple tension, simple torsion, and radial measurements with constant stress ratios  $\dot{\sigma}/\dot{S} = \text{constant}$  are shown in Fig. 1.

The data of Fig. 1 are plotted as  $T^2$  vs  $\Gamma$ , since in all of the experimental results for annealed copper at finite strain the generalized stress  $T$  and the generalized strain  $\Gamma$  are related parabolically, as indicated in eqn (1). From the observed straight lines in  $T^2$  vs  $\Gamma$  plots, one obtains a numerical value for the parabola coefficient,  $\beta$ . Significantly, the value of  $\beta$  thus

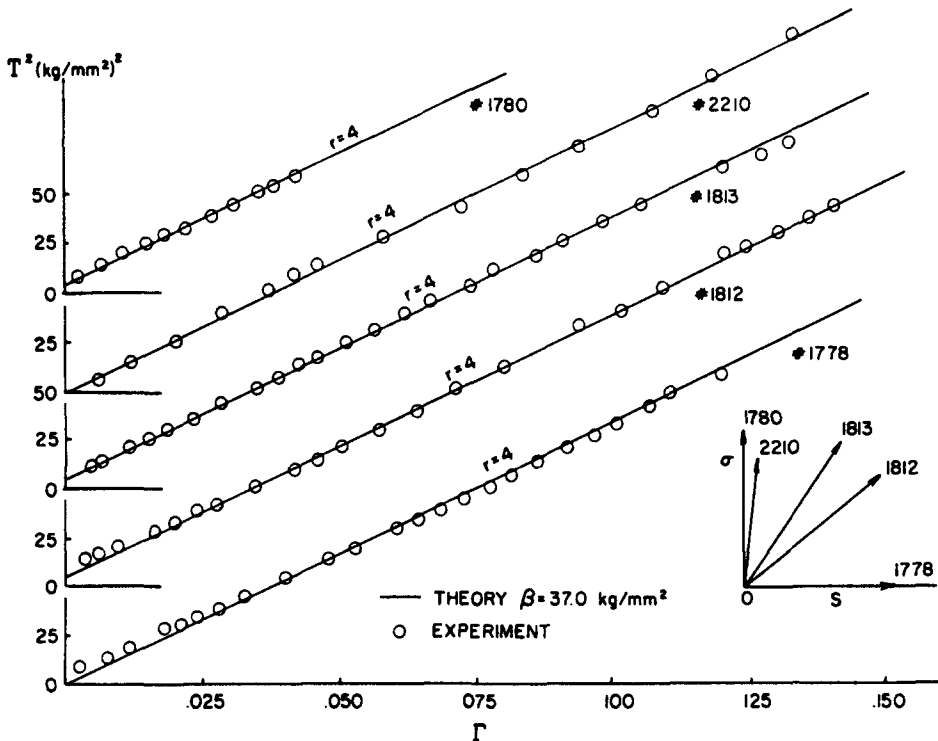


Fig. 1. Finite strain theory, eqn (1) (solid lines) compared with experiment (circles) for the proportional loading tests having the stress ratios shown.

determined is numerically the same for all types of loading histories; hence, one satisfies the first requirement for a general theory of finite strain plasticity based on experiment. There is both quantitative and qualitative order in the domain of finite strain.

For copper annealed in an oxygen free atmosphere for one hour and cooled in the furnace, the common parabola coefficient is  $\beta = 37.0 \text{ kg/mm}^2$  ( $5.26 \times 10^4 \text{ psi}$ ). It is interesting and of importance to finite strain theory that such a value of  $\beta$  was measured for annealed copper in 1962 in diffraction grating measurements of finite strain wave profiles [9] for strain rates of  $10^2$ – $10^3$ /sec. far higher (several million times higher) than those for the quasi-static tests of the present study,  $10^{-5}$ – $10^{-4}$ /sec.

In Fig. 2 are shown the  $\epsilon$  vs  $s$  measurements for two of the five radial, proportional loading tests, Nos 1813 and 2210 of Fig. 1, for which  $\dot{\sigma}/\dot{S}$  have the quite different constant values, 1.461 and 10.983, respectively.

The slopes  $\epsilon/s$  for Fig. 2 are given by the theory from the incremental strain vector  $d\epsilon/ds$  obtained from the ratio of eqns (2) and (3), i.e.  $d\epsilon/ds = \sigma/3S$ . From the constant ratios  $\dot{\sigma}/\dot{S}$  stated, the predicted values of  $d\epsilon/ds = \sigma/3S$  are 0.487 for test 1813, and 3.661 for test 2210. These slopes are given by the solid lines of Fig. 2, which illustrate the close correlation between theory and experiment for such finite strain measurements.

Because of path dependence in *non-proportional* loading,  $\Gamma$  may not be computed from the measurement of the finite strain components  $\epsilon$  and  $s$ . To illustrate how, for non-proportional loading one may ascertain whether or not the  $T$  vs  $\Gamma$  response is parabolic (eqn 1), with the common parabola coefficient  $\beta$ , it is sufficient to consider a test in which proportional loading to some defined point in stress space is followed by subsequent loading to large finite strain along a continued stress path in either  $\sigma$  or  $S$  alone. For example, a thin-walled annealed copper tube is loaded in simple tension to a prescribed value of tensile stress  $\sigma_0$ . With this stress held constant, a torsion load is applied to large finite strain. For the finite strain domain in which  $\sigma_0$  is constant, eqn (2) becomes eqn (6).

$$\frac{dT}{d\epsilon} = \frac{3\beta^2}{4\sigma_0} \quad (6)$$

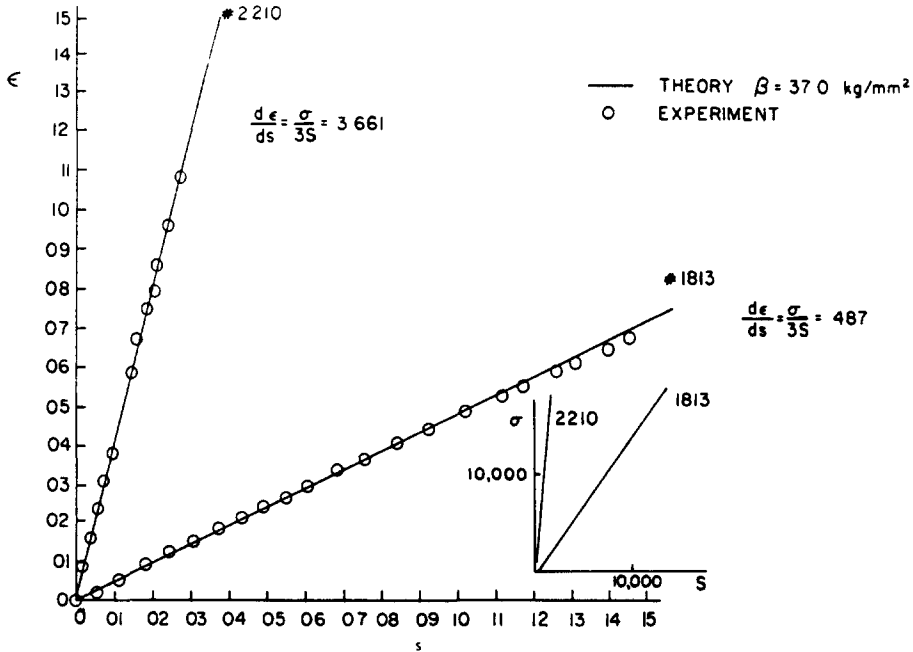


Fig. 2. The finite strain theory (solid lines) of eqns (4) and (5) compared with experiment (circles) for proportional loading.

Thus, in a  $T$  vs  $\epsilon$  plot, the slope should be constant. Knowing  $\sigma_0$ , measurement of the slope will provide the value of  $\beta$ . Such experimental data are shown in Fig. 3. The circles are the measured experimental data and the solid line is that predicted from the value of  $\beta$  obtained in proportional loading tests in similar annealed copper tubes. The fact that the data lie along a straight line indicates not only the presence of parabolicity in finite deformation but also the applicability of the incremental theory of finite strain to non-proportional loading.

With parabolicity established and the value of  $\beta$  measured during the non-proportional loading test, we may readily integrate the shear strain in eqn (3) to compare the known value of

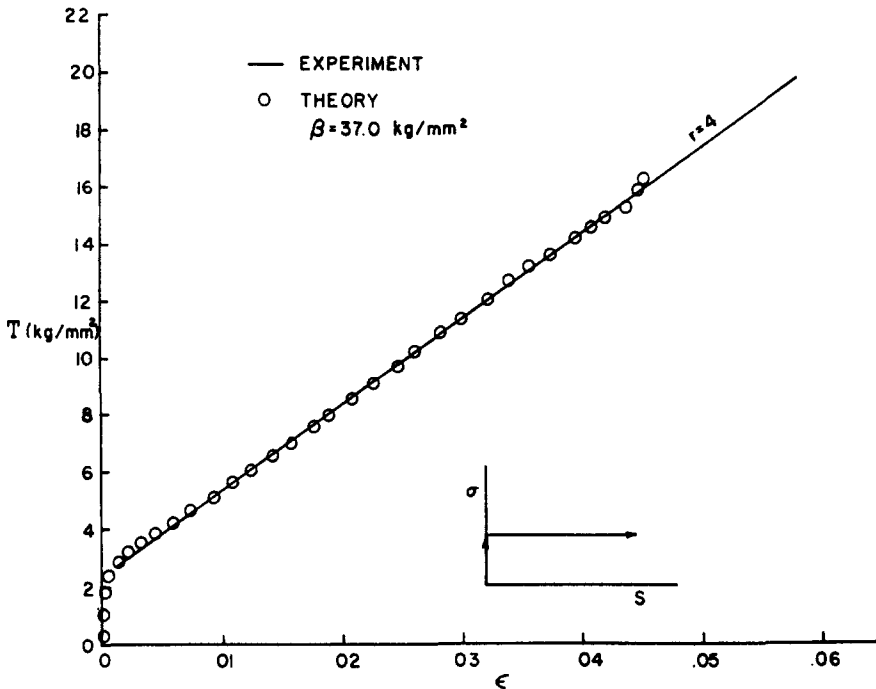


Fig. 3. A comparison of theory (solid line) and experiment (circles) for the predicted constant slope of eqn (6) in non-proportional loading. (Test 2211).

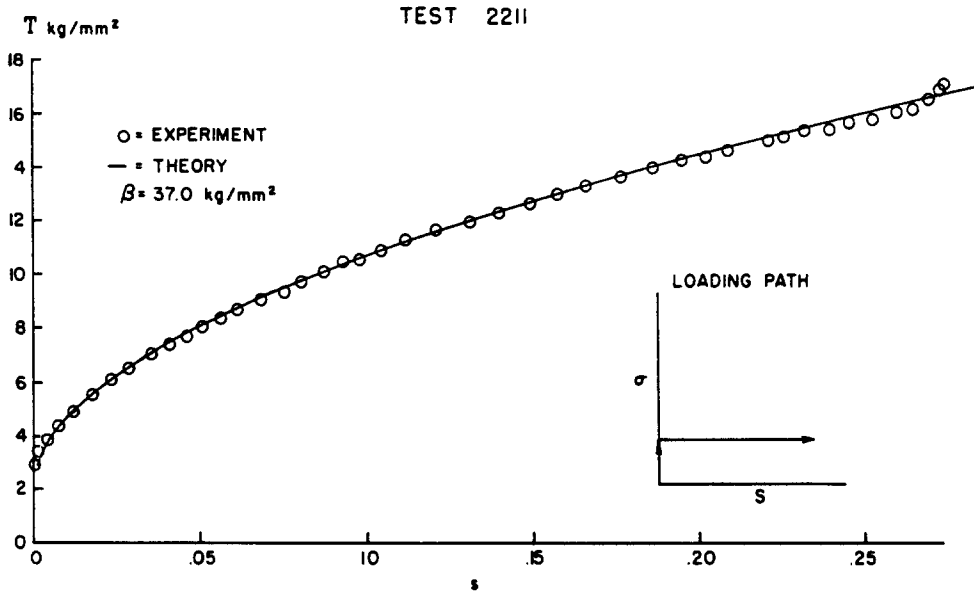


Fig. 4. The T vs s plot of prediction from the integration of eqn (3) for the non-proportional path shown (solid line) compared with measurement (circles).

T with the measured value of s. Such a comparison is shown in Fig. 4 for finite shear strains to 27%.

From these results one may integrate for the path dependent, generalized strain  $\Gamma$ , thereby obtaining the correlation between the theory of finite strain (solid line) and experiment for the parabolicity of eqn (1), as shown in the T vs  $\Gamma$  plot of Fig. 5.

Proceeding in such a manner, we studied the finite strain response to the different non-proportional loading paths shown in Fig. 6.

In Fig. 7 are shown T<sup>2</sup> vs  $\Gamma$  plots for a cross-section of these experiments. The value of  $\Gamma$  was obtained as described above for non-proportional loading. The solid lines are the theoretical slopes given by the value of the parabola coefficient,  $\beta = 37.0 \text{ kg/mm}^2$  ( $5.26 \times 10^4 \text{ psi}$ ) obtained from proportional loading tests such as those shown in Fig. 1 and from non-proportional tests as shown in Fig. 3.

With the loading path given, it is a simple matter to integrate the constitutive statements of

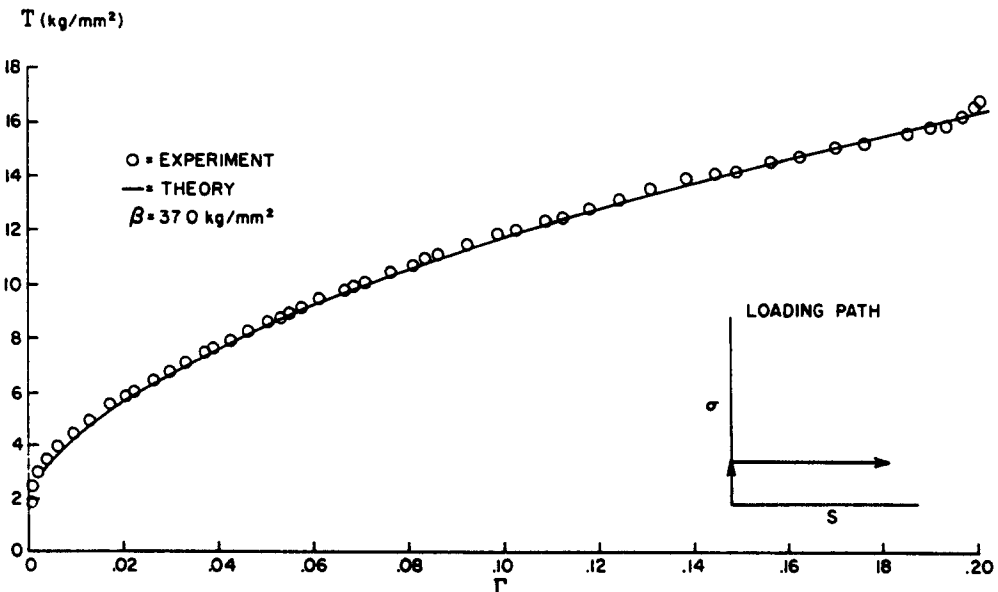


Fig. 5. A T vs  $\Gamma$  plot of the parabolic deformation for  $\beta = 37.0 \text{ kg/mm}^2$  (solid line) compared with experiment (circles) in which the path dependence of  $\Gamma$  is included. (Test 2211).

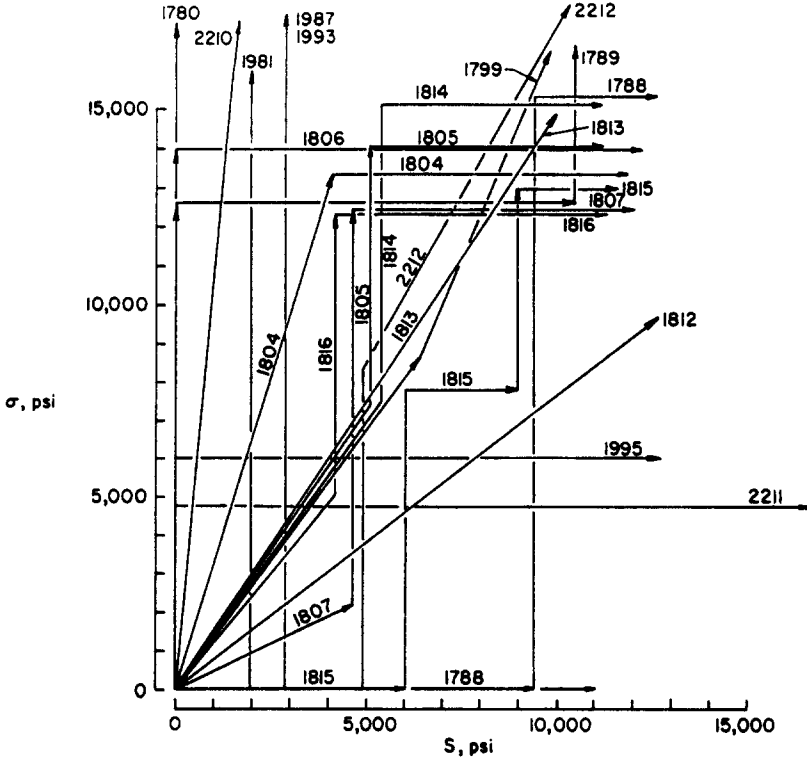


Fig. 6. Diagrams in stress space of a cross-section of the proportional and non-proportional loading paths considered in this study.

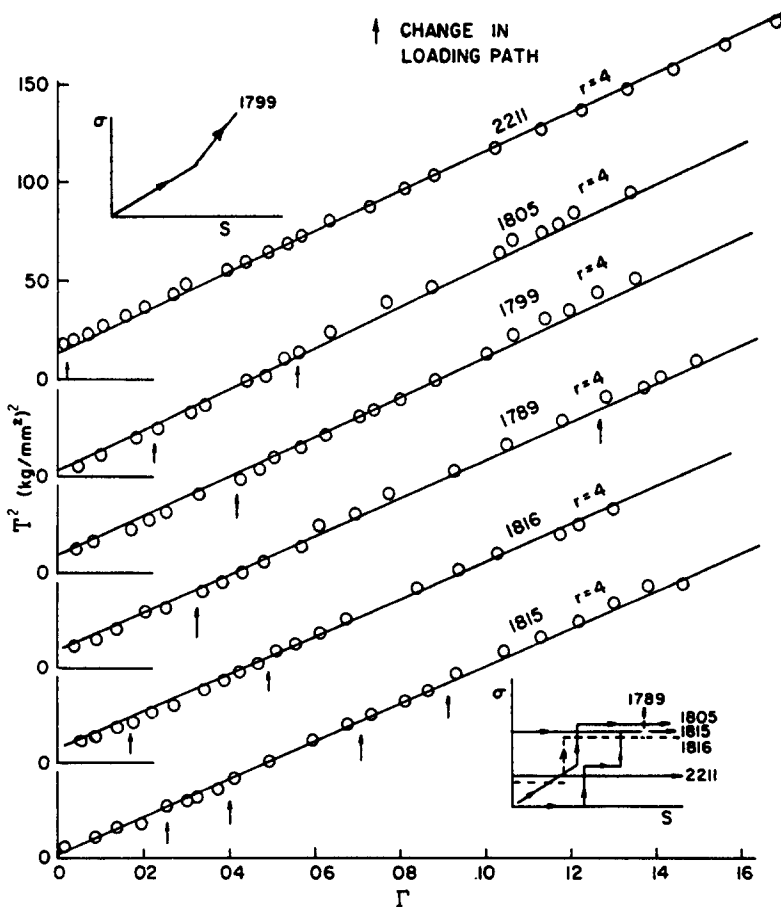


Fig. 7.  $T^2$  vs  $\Gamma$  plots of representative non-proportional loading tests in which the path dependence of  $\Gamma$  is included. The observed parabolicity of the theory (solid line) is for  $\beta = 37.0 \text{ kg/mm}^2$  in each instance.

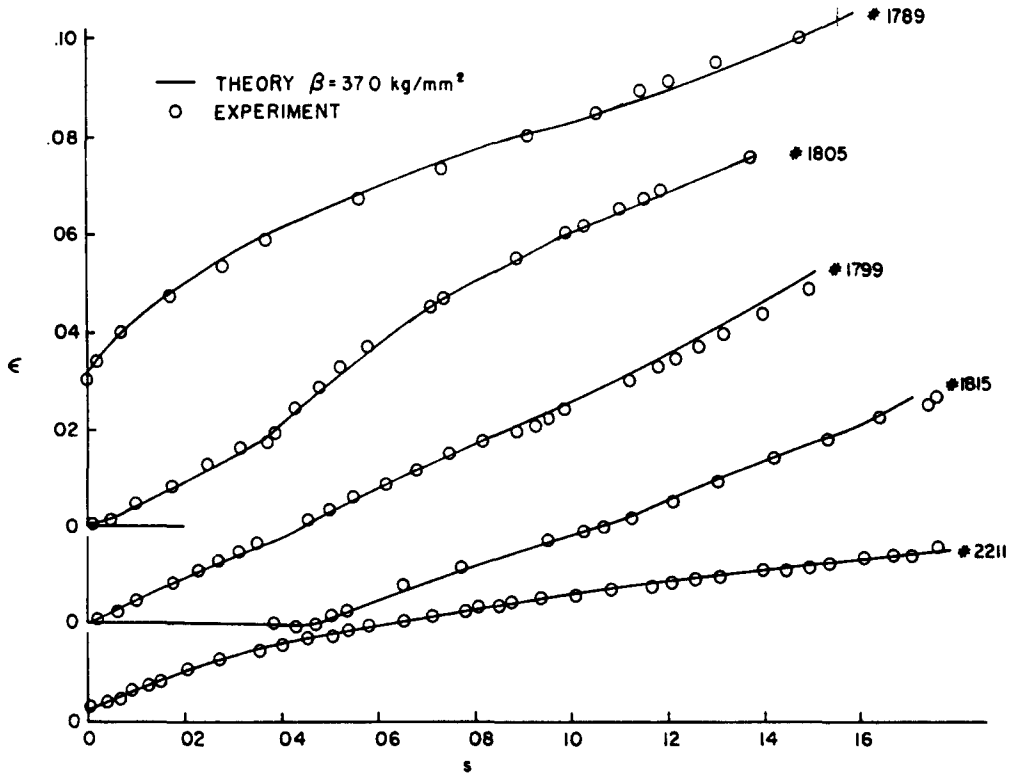


Fig. 8. Experimental results in strain space compared with prediction from the incremental finite strain theory by the integration of eqns (2) and (3), with  $\beta = 37.0 \text{ kg/mm}^2$ .

eqns (2) and (3) in each instance. Such comparisons of finite strain theory (solid lines) and experiment are shown in the  $\epsilon$  vs  $s$  strain plots of Fig. 8.

#### THE INCREMENTAL THEORY OF FINITE STRAIN VS A DEFORMATION THEORY APPROXIMATION

The correlation between an incremental finite strain theory and experiment which we have shown here is important because it parallels that which Bell obtained from similar studies in several other metals and metal alloys [1, 4-8]. A second and equally important motivation for the present study has been to choose non-proportional loading paths which would test the degree of approximation obtainable from earlier deformation theories when compared with the exact, incremental finite strain theory and experiment.

In proportional loading tests of the type described above, eqns (2) and (3) readily may be integrated to provide constitutive statements of the deformation type, eqns (4) and (5). As is expected, incremental and deformation theories coincide for proportional loading. The use of eqns (4) and (5) for non-proportional loading permits a direct examination of the difference between incremental and deformation theory predictions as a function of variations in non-proportional loading.

Pursuit of this comparison did not rise entirely from an interest in the historical debates over incremental vs deformation theories aroused by the experimental studies of many decades ago. It was prompted also by the realization that it would be advantageous for practical technology if bounds could be established for domains of non-proportional loading paths in which the much simpler, easily converted, deformation type constitutive statements could give results within engineering approximation.

In Fig. 9 are shown the results of calculations for the incremental theory obtained by the integration of eqns (2) and (3) (solid lines) and those obtained by assuming the deformation statements of eqns (4) and (5) (dashed lines). The correlation between the incremental theory of finite strain (solid lines) and experimental observation in strain space (circles) was shown in Fig. 8 for these same non-proportional tests.

In every instance, whatever by the angle at the change of path, the incremental theory of

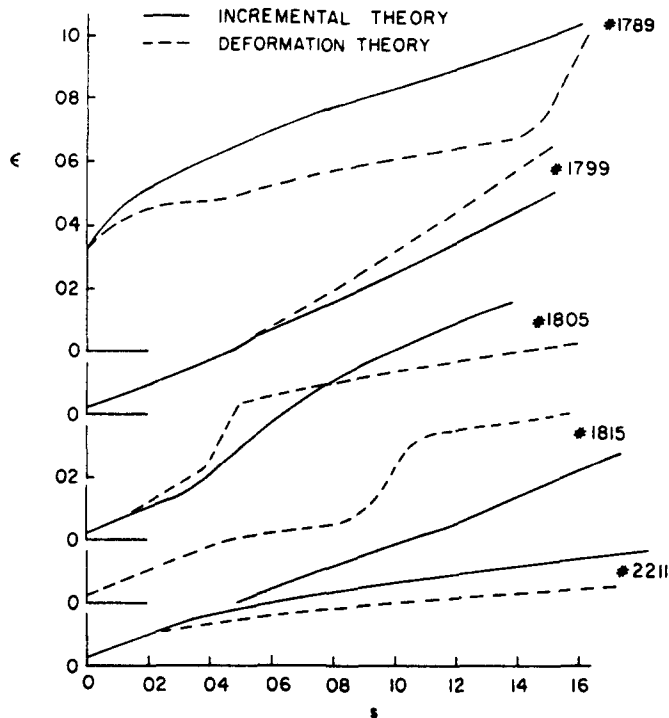


Fig. 9. Strain space plots from the integration of eqns (2) and (3) from the incremental finite strain theory for the non-proportional loading tests in Fig. 8, compared with results from a deformation theory approximation, eqns (4) and (5).

finite strain is found to be in close correlation with experiment. For the straight line segments considered in the non-proportional loading paths of Fig. 6, the integrals obtained from eqns (2) and (3) are standard forms and thus are easily integrated. An inspection of Fig. 9 reveals, as one would anticipate, the predictions of the deformation theory are widely divergent for a  $90^\circ$  corner. This is particularly true when the individual test undergoes a series of  $90^\circ$  alterations in path directions such as that shown for test 1815.

What is more surprising, however, is the result obtained for test 1799 in which a radial path for which  $\dot{\sigma}/\dot{S} = 1.33$  undergoes a change in the middle of the test to a constant ratio  $\dot{\sigma}/\dot{S} = 2.28$ . Since the first slope is  $53^\circ$  and the second slope is  $66^\circ$ , the angular change is only  $13^\circ$ . As may be seen in Fig. 9, even for such a relatively small change in path direction, during finite strain the deformation theory calculation still gives a poor approximation.

We thus may conclude that in general it is essential to have recourse to an incremental theory of finite strain in non-proportional loading. The degree of error introduced by the deformation theory depends not only upon the magnitude of the angular change but also upon the values of the stress components  $\sigma_0$  and  $S_0$  when the change occurs. On introducing a  $90^\circ$  corner along either the tensile or torsion axes, the degree of error in the deformation theory decreases as the stress  $\sigma_0$  or  $S_0$  decreases. A study of many such non-proportional tests over a range of tests with  $90^\circ$  corners which include very small values of constant stress, has shown that the error in the deformation theory prediction always is considerable, while the incremental theory of finite strain always is in close accord.

Nearly a decade ago, in the first series of non-proportional loading experiments in the context of parabolic plasticity [4], the values of  $\sigma_0$  and  $S_0$  were relatively small. It appeared at that early point that some question might be raised with respect to the choice of theory. Several metals and several hundred tests later, the answer to such a question is definitive, namely, that the finite strain plasticity of metals must be described in terms of an incremental theory.

One other type of finite strain test is of interest, one in which a non-proportional loading path including a  $90^\circ$  corner is brought to a stress  $\sigma_1$  and  $S_1$ , following which the loading path is in proportional loading from the origin. Such a situation is provided in the results of test 2212 in which simple torsion is first applied for 26 min at a constant stress rate of  $\dot{S} = 0.13 \text{ kg/mm}^2/\text{min}$ . Subsequently the shear stress of  $S_0 = 3.50 \text{ kg/mm}^2$  is held constant while the tensile stress is



applied at a constant stress rate of  $\dot{\sigma} = 0.23 \text{ kg/mm}^2/\text{min}$ , also for 26 min. At the end of the second interval the tensile stress is continued and the shear stress is again introduced at the same stress rate. This results in a proportional loading path following what had been a very non-proportional loading history. In both non-proportional and proportional loading sections the parabolicity of eqn (1) is applicable, with the common parabola coefficient of  $\beta = 37.0 \text{ kg/mm}^2$  ( $5.26 \times 10^4 \text{ psi}$ ).

For the strain path shown in Fig. 10, the incremental theory (solid line) and experimental results are seen to be in close agreement in both the proportional and non-proportional sections of the test. These are compared with the calculation of a deformation type response from the origin (dashed line).

Thus again, the incremental theory of finite strain describes with close precision the deformation, while the degree of approximation of deformation type response functions varies with the detail of the non-proportional loading paths which precedes the introduction of a proportional loading section.

Finally, for this test a plot of  $T$  vs  $s$  illustrated the close accord between incremental finite strain theory, eqn (3) and experiment for shear strains,  $s$ , as high as 28%. Bell has commented elsewhere [7] at some length upon the fact that the shear strain  $s$  is defined as  $s = r_m \theta / l_0$  whether in simple torsion or in the presence of finite tensile strains of over 12%, as in test 2212.

#### A GENERALIZATION FOR THE MEASURED MATERIAL CONSTANT, $\beta$

In the present discussion it is pertinent to point out that the parabola coefficient  $\beta = 37.0 \text{ kg/mm}^2$  ( $5.26 \times 10^4 \text{ psi}$ ), obtained for the finite straining of annealed copper, is itself derivable from broader studies of the fundamental physics. The strain rates of the quasi-static tests described here are in the range of  $10^{-4}/\text{sec}$ . The numerical value of parabola coefficients of  $\beta$  were first obtained nearly twenty years ago by Bell [10, 11] at the high strain rates of plastic wave propagation in diffraction grating measurements of finite strain wave profiles in compression. Khan [12, 13] in the first diffraction grating measurements of finite strain during the propagation of plastic *tensile* waves showed that not only was the response function for tensile waves parabolic, but also that the parabola coefficient obtained was identical with that obtained for compression.

In both the compression experiments and the tensile experiments on the propagation of plastic waves, the strain rates were between  $10^2/\text{sec}$ . and  $10^3/\text{sec}$ . at finite strain, i.e. a range of strain rates of  $10^7$  when compared with quasi-static tests such as those of the finite strain

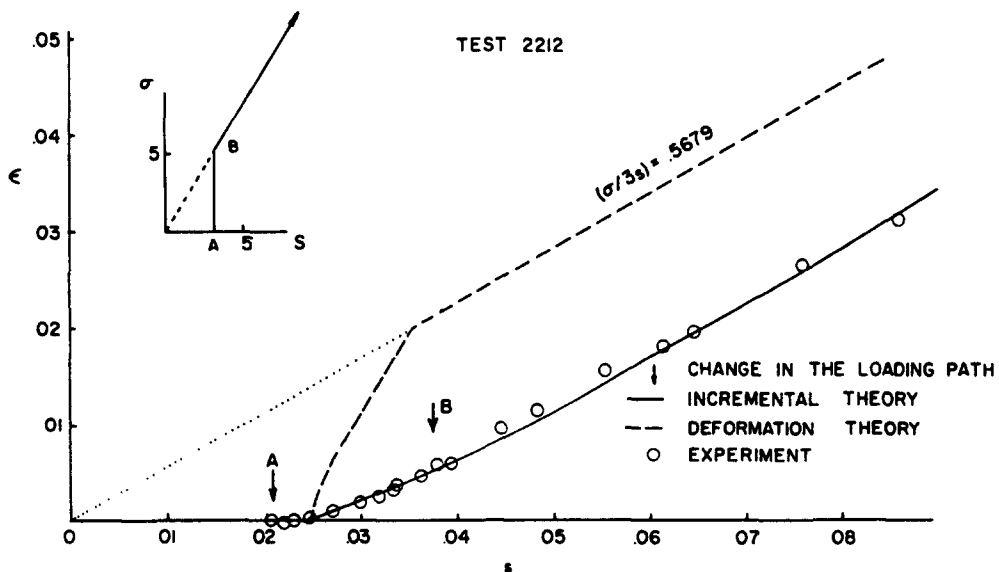


Fig. 10. Experiment (circles) and incremental finite strain theory following integration of eqns (2) and (3) (solid line) compared to a deformation theory, eqns (4) and (5) (dashed line). In this test, proportional loading follows rather than precedes non-proportional loading.

experiments of the present paper. The value of the material constant  $\beta$  for finite strain is thus sensibly strain rate independent.

The finite amplitude wave studies in several metals in the early 1960s provided the genesis for years of systematic analysis of both polycrystalline and related single crystalline response functions which were collated in a monograph [11] in 1968 and summarized in a *Handbuch der Physik* [1] treatise in 1973. Knowing the value of  $u(0)$ , the shear modulus at absolute zero; the ambient temperature  $T^\circ\text{K}$ ; the melting point  $T_m^\circ\text{K}$ ; a dimensionless universal constant  $B_0 = 0.0207$  common to 50 crystalline solids; and a characteristic deformation mode index,  $r = 1, 2, 3, 4, \dots$ ; the parabola coefficient for any crystalline solid of the class may be calculated from eqn (7).

$$\beta = \left(\frac{2}{3}\right)^{r2} u(0)B_0(1 - T/T_m). \quad (7)$$

For annealed copper,  $u(0) = 5148 \text{ kg/mm}^2$ ,  $T = 298^\circ\text{K}$ ,  $T_m = 1358^\circ\text{K}$ . For a deformation mode index of  $r = 4$ , one obtains from a unified structure for ordered solids, the specific parabola coefficient,  $\beta = 37.0 \text{ kg/mm}^2$  ( $5.26 \times 10^4 \text{ psi}$ ), found in all the present finite strain tests. As Bell has shown in the historical survey of finite strain data published in the literature from the mid-19th century to the present, this deformation mode index of  $r = 4$  has been nearly universally observed for annealed copper.

Equation (7), which applies here to the annealed copper experimental data, may be used to determine the applicable parabola coefficient of each of the many different crystalline solids—annealed metals, metal alloys, rock salt and nylon 6—from ambient temperatures in the vicinity of absolute zero to within  $90^\circ$  of the melting point, as finite strain experiments of the past two decades have amply demonstrated.

#### SUMMARY

The general theory of finite strain plasticity which applies to a wide variety of ordered solids is considered here specifically with regard to annealed copper. Any experiment designed to examine such a theory requires a detailed study of the domain of non-proportional loading paths where path changes are sufficiently drastic to provide a proper test of the applicability of the theory. It is of no small significance that the experiments considered here are for dead-weight loading, and in that respect differ from many of the experiments reported in the literature. In dead-weight loading, the stress components are prescribed and the measured quantities are the resulting strains, a decided contrast to hard testing machines in which the strains or strain rates are imposed and the stresses become the measured quantities.

Of importance, too, the design of the present tension-torsion apparatus was such that the tensile strain  $\epsilon$  and the torsion strain  $s$  were decoupled. No constraint was imposed in torsion since the tensile load did not rotate during deformation.

For finite strain during non-proportional loading, a comparison is made between an incremental theory and a deformation theory. The deformation theory is one which coincides with the incremental theory during proportional loading. For both proportional and non-proportional loading, experiment is in accord with the incremental theory. There is a large degree of error in the deformation theory approximation during non-proportional loading. This is true even for small alterations in the proportional loading path.

In sum, the incremental theory of finite strain parabolic plasticity is shown to be in very close agreement with experiment in annealed copper for arbitrary proportional and non-proportional loading paths for which  $dT \geq 0$  for strain components as high as, or even greater than, 30% deformation.

#### REFERENCES

1. J. F. Bell, The experimental foundations of solid mechanics. *Handbuch der Physik*, Vol. VIa/1. Springer-Verlag, New York (1973).
2. R. Mittal, Biaxial loading of aluminum and a generalization of the parabolic law. *J. Mat.* 6, 67 (1971).
3. H. Moon, An experimental study of incremental response functions in the totally plastic region. *Acta Mechanica* 23, 49 (1975).
4. J. F. Bell, The experimental foundations of solid mechanics. *Handbuch der Physik*, Vol. VIa/1, Section 4.35. Springer-Verlag, New York (1973).

5. J. F. Bell, A new, general theory of plasticity for structural metal alloys. BRL Contract Report No. 250, The Johns Hopkins University, Baltimore (1975).
6. J. F. Bell, Origins in experiment of a new general theory of plasticity for structural metal alloys. BRL Contract Report No. 311, The Johns Hopkins University, Baltimore (1976).
7. J. F. Bell, A physical basis for continuum theories of finite strain plasticity: Part I. *Archive for Rational Mechanics and Analysis* (in press).
8. J. F. Bell, A physical basis for continuum theories of finite strain plasticity: Part II. *Archive for Rational Mechanics and Analysis* (in press).
9. J. F. Bell and W. M. Werner, Applicability of the Taylor theory of the polycrystalline aggregate to finite amplitude wave propagation in annealed copper. *J. Appl. Phys.* 33(8), 2416 (1962).
10. J. F. Bell, Propagation of large amplitude waves in annealed aluminum. *J. Appl. Phys.* 31(2), 277 (1960).
11. J. F. Bell, *The Physics of Large Deformation of Crystalline Solids. Springer Tracts in Natural Philosophy*, Vol. 14. Springer-Verlag, New York (1968).
12. A. S. Khan, A study of one dimensionality and isochoric deformation during the passage of tensile waves. *Experimental Mech.* 14(2), 57 (1974).
13. A. S. Khan, Behavior of aluminum during the passage of large-amplitude plastic waves. *Int. J. Mech. Sci.* 15, 503 (1973).